Testing an optical window of a small wedge angle: effect of multiple reflections

Chiayu Ai and James C. Wyant

Multiple reflections between two surfaces of a window introduce a fixed pattern error in optical measurements. One way to remove these spurious reflections is to use a reasonably large wedge so that the interference fringes formed by the two surfaces are too dense for the detector to resolve. However, this method does not work if the wedge angle is small, e.g., several arcseconds. By tilting both the window and the return mirror properly, it is possible to remove the effect of multiple reflections of a window. Theory and experimental results are presented.

Key words: Optical testing, optical window, multiple reflection.

Introduction

Spurious reflections usually introduce errors into the measurement results obtained with laser phase-shifting interferometry.[1–7] For a Fizeau interferometer, work has been done to reduce or eliminate the effect of the multiple reflections between the test and reference surfaces. For example, Hariharan[3] points out that if a four-frame phase calculation algorithm is used, the phase error caused by multiple reflections is eliminated to a first-order approximation. Bonsch and Bohme[5] give a new algorithm that can completely eliminate the phase error resulting from multiple reflections of a test mirror. We show the phase error caused by the multiple reflections from a retroreflection.[7]

When testing a window, one always tilts it to keep direct reflections from the two surfaces of the window from entering the interferometer. However, multiple reflections between two surfaces of a window introduce an error of a fixed pattern in the measurement result, no matter what the window tilt angle and the window thickness. One way to remove the effect of these spurious reflections is to have a reasonably large wedge angle in the window such that the interference fringes formed by the two surfaces are too dense for the detector to resolve. However, this method does not work if the wedge angle is only several arcseconds. In this paper, we present the theory and results of the experiments we have performed with windows of a small wedge angle.

The authors are with Wyko Corporation, 2650 East Elvira Road, Tucson, Arizona 85706.

Received 3 November 1992.
0003-6935/93/254904-09$06.00/0.

Theory

For a planar parallel plate or optical window, the relative amplitudes of the successive internally reflected rays are 1, r^2, r^4, . . . , where r is the coefficient of reflection of the window. If the incident angle is θ, it can be shown that the optical path difference (OPD) of two successive rays is equal to $2dn\cos(\theta')$, where d and n are the thickness and the refractive index of the window, respectively, and θ' is the refractive angle. For a more general case, dn is the optical thickness or the integration of the length times the refractive index along the path. For a small incident angle, the coefficient of reflection, r, of most optical glass is about 20%. Therefore the multiple reflections of a window can be approximated by the first two rays, i.e., 1 and r^2.

When testing an optical window, a collimated beam is incident upon the window. The transmitted wave can be approximated by two rays, 1 and r^2. These two rays are reflected back to the window by the return flat (RF), which has a coefficient of reflection of s, as shown in Fig. 1. Between the window and the RF, the filled-arrow ray has a relative amplitude of s, and the open-arrow ray has a relative amplitude of r^2s. In the following we show that the tilt of the RF can alter the effect of the multiple reflections on the phase measurement. For convenience, we discuss this effect for two cases: (1) a ray normal to the RF and (2) a tilted RF.

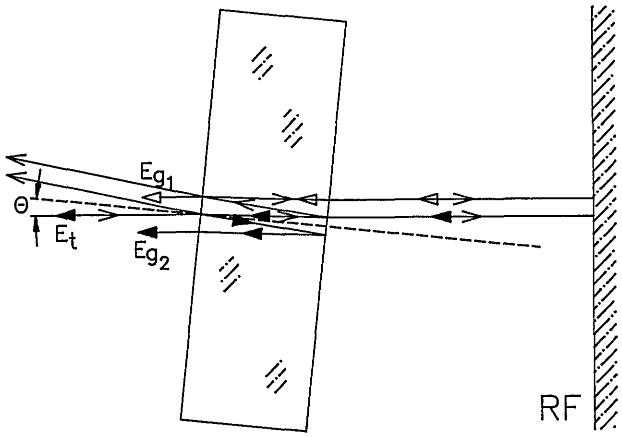

Fig. 1. Ray path through a window and reflected by a return flat (RF). The window is tilted of an angle θ.

Normal to the RF

From Fig. 1, each of the two reflected rays has multiple reflections inside the window. The multiple reflections of the filled-arrow ray in the window can be approximated by the first two rays, E_t and E_{g2}. Because of the low reflectivity of the window, the multiple reflections of the opoen-arrow ray in the window are negligible; only the transmitted ray E_{g1} is significant. Therefore for an incident ray from the source entering the window, there are three returned rays, E_t, E_{g1}, and E_{g2}, as shown in Fig. 1. Because of the nonzero incident angle, the returned rays E_{g1} and E_{g2} are laterally displaced from the original incident location by approximately $d\theta(1 - 1/n)$ and go through different regions of the window, x_1 and x_2, respectively. If the thicknesses of the two regions are d_1 and d_2, respectively, the complex amplitudes of the three rays are

$$\begin{aligned} E_t &= s \exp \mathbf{i}[2\phi_w(x,y) + \phi_r(x,y)], \\ E_{g1} &= r^2 s \exp \mathbf{i}[\phi_w(x,y) + \phi_w(x_1,y) + \phi_r(x,y) \\ &\quad + 2d_1 n \cos(\theta')k], \\ E_{g2} &= r^2 s \exp \mathbf{i}[\phi_w(x,y) + \phi_w(x_2,y) + \phi_r(x,y) \\ &\quad + 2d_2 n \cos(\theta')k], \end{aligned} \tag{1}$$

where $k = 2\pi/\lambda$ and θ' is the refracted angle inside the window. The $\phi_w(x, y)$ and $\phi_r(x, y)$ are the contributions of the window and the RF, respectively. For a small incident angle θ, the lateral displacement $d\theta(1 - 1/n)$ is negligible, i.e., $x_1 \approx x_2$. Therefore the three returned rays, E_t, E_{g1}, and E_{g2}, are close to each other and can be approximated by the location of the returned ray, E_t. Because the two reflected rays are normal to the RF, the location of these three returned rays is close to the original incident ray location x on the window. If the RF is tilted, these three rays deviate from the location x, as discussed in the next section.

If the optical thickness $d(x, y)n$ is a constant over the entire window, we can substitute $\phi_w(x_1, y)$ and $\phi_w(x_2, y)$ with $\phi_w(x, y)$, and both d_1 and d_2 with $d(x, y)$, and the sum of the three rays is

$$\begin{aligned} E_t + E_{g1} + E_{g2} &= s \exp \mathbf{i}[2\phi_w(x,y) + \phi_r(x,y)] \\ &\quad \times \{1 + 2r^2 \exp \mathbf{i}[2d(x,y)n \cos(\theta')k]\}. \end{aligned} \tag{2}$$

For a given incident angle θ, the term inside the curved brackets is a constant over the entire window. Thus the phase of the resulting wave front is determined by $2\phi_w(x, y) + \phi_r(x, y)$. The multiple reflections have no effect on the measurement. However, in reality, the optical thickness $d(x, y)n$ is not equal to a constant over the window. For example, a change in $d(x, y)n$ as small as 0.25λ can produce a large change in the phase of $1 + 2r^2 \exp \mathbf{i}[2d(x, y)n \cos(\theta')k]$. In all, when the RF is normal to the ray, the vector sum of the three rays varies with the optical thickness of a window along its wedge direction, and hence the resulting wave front and the measurement result have ripples perpendicular to the wedge direction.

Tilting the RF

In the above discussion, the rays are normal to the RF. The two reflected rays follow the original ray path. However, if the RF is tilted at an angle ϵ, the returned ray E_t deviates from the original location x to x' on the window. When both the window and the RF are tilted in the same direction, the incident angle of the returned ray is $\theta - 2\epsilon$. If they are tilted in opposite directions, the incident angle is $\theta + 2\epsilon$, as shown in Fig. 2. Because the three returned rays are close to each other, we use x' to represent their locations on the window, and the distance of $x' - x$ is defined as the walk-off distance. For simplicity, we assume that the lateral displacement is smaller than the walk-off distance. It can be shown that the OPD between two successive rays for E_{g2} is equal to $2d(x', y)n \cos(\theta'')$, where θ'' is the corresponding refracted angle for the incident angle of either $\theta - 2\epsilon$ or $\theta + 2\epsilon$, depending on the tilt directions. Therefore the complex amplitudes of the three returned rays are

$$\begin{aligned} E_t &= s \exp \mathbf{i}[\phi_w(x,y) + \phi_w(x',y) + \phi_r(x,y)], \\ E_{g1} &= r^2 s \exp \mathbf{i}[\phi_w(x,y) + \phi_w(x',y) + \phi_r(x,y) \\ &\quad + 2d(x,y)n \cos(\theta')k], \\ E_{g2} &= r^2 s \exp \mathbf{i}[\phi_w(x,y) + \phi_w(x',y) + \phi_r(x,y) \\ &\quad + 2d(x',y)n \cos(\theta'')k], \end{aligned} \tag{3}$$

It should be noted that for E_{g1} the multiple reflections occur at x not x', and hence the OPD between two successive rays is equal to $2d(x, y)n \cos(\theta')$, not $2d(x', y)n \cos(\theta'')$. Mainly because of the change in the incident angle, the value of $2d(x', y)n \cos(\theta'')$ is different from that of $2d(x, y)n \cos(\theta')$. This makes it possible to cancel E_{g1} and E_{g2} and eliminate the effect of multiple reflections. The sum of the three

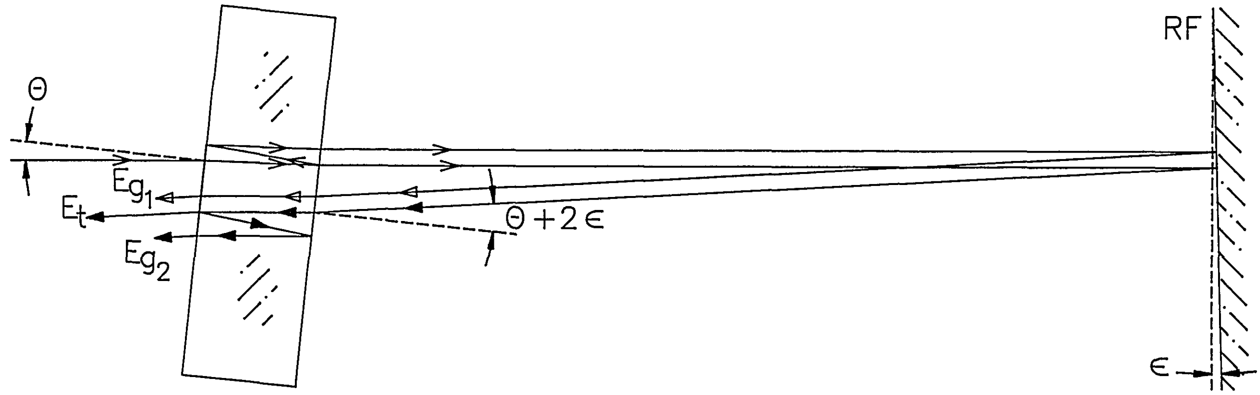

Fig. 2. Ray path similar to Fig. 1, except the RF is tilted by an angle ϵ. The reflected ray deviates from the original location. Here the RF is away from the window to show the ray deviation. This deviation can be reduced by moving the RF closer to the window.

rays is

$$E_t + E_{g1} + E_{g2} = s \exp \mathbf{i}[\phi_w(x,y) + \phi_w(x',y) + \phi_r(x,y)] \times \{1 + r^2 \exp \mathbf{i}[2d(x,y)n\cos(\theta')k] + r^2 \exp \mathbf{i}[2d(x',y)n\cos(\theta'')k]\}, \quad (4)$$

where

$$\theta' = \cos^{-1}\{[1 - \sin^2(\theta)/n^2]^{1/2}\},$$
$$\theta'' = \cos^{-1}\{[1 - \sin^2(\theta - 2\epsilon)/n^2]^{1/2}\}. \quad (5)$$

From Eq. (4), we can see that the resulting wave front is modulated by E_{g1} and E_{g2}. Because the three rays have the same polarization, they can be manipulated as phasors. It can be shown that the error caused by multiple reflections is determined by the magnitude and the angle of the sum phasor, $E_{g1} + E_{g2}$, as shown in Fig. 3. In the following, we refer frequently to this sum phasor. The angle between the phasors E_{g1} and E_{g2} is important in determining the magnitude of the sum phasor. For convenience, we define a quantity φ as the angle between E_{g1} and E_{g2} and L as the magnitude of the sum phasor, $E_{g1} + E_{g2}$. Because E_{g1} and E_{g2} have the same magnitude, φ and L can be

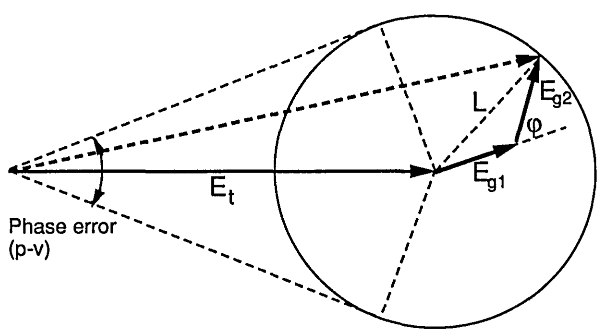

Fig. 3. Sum of three phasors, $E_t + E_{g1} + E_{g2}$. The magnitude (L) and the angle (φ) of the sum phasor, $E_{g1} + E_{g2}$, determines the error caused by the multiple reflections. The phase error (p–v) = $|2\sin^{-1}(L/|E_t|)|$ in radians.

expressed as follows:

$$\varphi = 2d(x,y)n\cos(\theta')k - 2d(x',y)n\cos(\theta'')k,$$
$$L = 2r^2 s|\cos(\varphi/2)|. \quad (6)$$

It is clear that the phase error is extreme when the sum of three rays is tangent to the circle of a radius L, as shown in Fig. 3. The two extremes of the errors are $+/-\sin^{-1}(L/|E_t|)$ in radians. Therefore the peak-to-valley value (p–v) of the phasor error is

$$\text{Phase error (p–v)} = |2\sin^{-1}[2r^2\cos(\varphi/2)]| \text{ in radians}$$
$$= |\sin^{-1}[2r^2\cos(\varphi/2)]/\pi| \text{ in fringes.} \quad (7)$$

Therefore (a) when φ = oddπ, both L and the error are zero, and (b) when φ = evenπ, $L = 2r^2 s$ and the error is maximum. If the coefficient of the reflection is ~20%, i.e., $r^2 = 4\%$, then the phase error $(p\text{–}v)$ = 0.0254 fringe. Figure 4 shows that L is a function of the tilt angle ϵ of the RF for different thicknesses.

For simplicity, we assume that the walk-off is negligible or that the window has an equal thickness in the direction of the walk-off, e.g., the x direction. Hence $d(x,y) = d(x',y) = d$. Using Eqs. (5) and (6), we obtain

$$\varphi = 2dnk\{[1 - \sin^2(\theta)/n^2]^{1/2} - [1 - \sin^2(\theta - 2\epsilon)/n^2]^{1/2}\}. \quad (8)$$

It is important to note that because the term in the curved bracket is a very small number, a small change in thickness does not change the value of φ. The values of L and φ are listed in Table 1 for different tilt angles θ and ϵ, where $n = 1.5$, $\lambda = 633$ nm, and $d = 10$ mm or 20 mm. It should be noted that whenever ϵ = 0°, φ always equal zero, regardless of the tilt and the thickness of the window. For this case, the error is maximum, unless the variation of the optical thickness over the entire window is much less than 1λ.

If $\epsilon \neq 0°$, φ can be any value according to Eq.

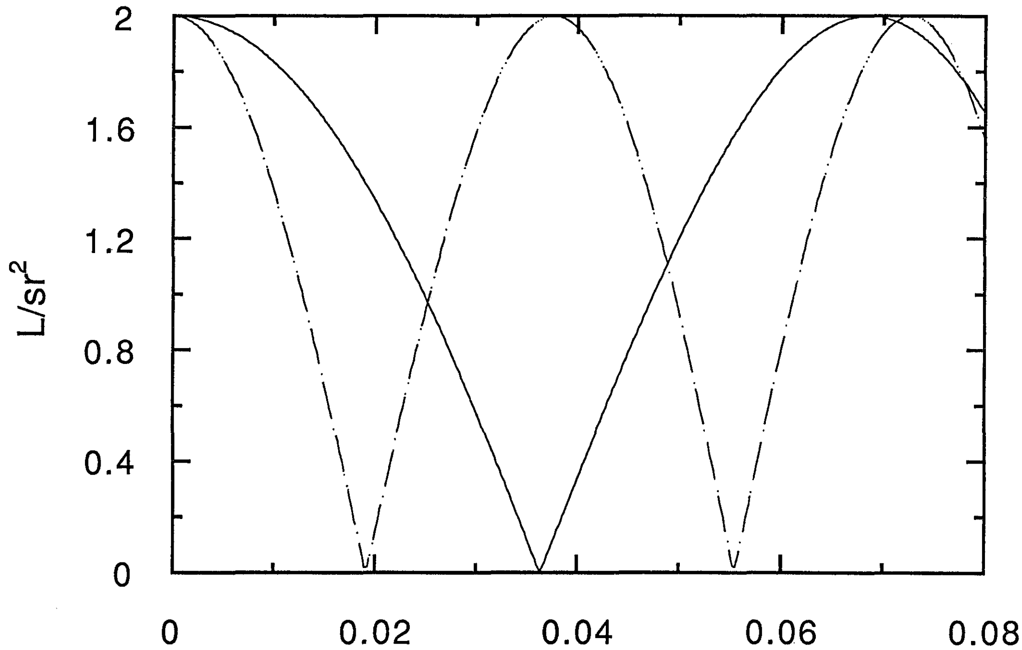

Fig. 4. L/sr^2, a function of ϵ (in degrees), for $d = 20$ mm, $n = 1.5$, $\lambda = 633$ nm, and $\theta = 0.5°$ (solid curve) and 1° (dashed curve).

(8). For a given θ and ϵ, a slight increment in the window thickness, e.g., $\Delta d = 2\lambda$, increases the OPD between two successive internally reflected rays by $2\Delta dn$, i.e., 6λ. The angle of each phasor E_{g1} and E_{g2} increases by 12π for $n = 1.5$. Because the angles of both phasors E_{g1} and E_{g2} increase by the same amount, the angle of the sum phasor also increases by 12π. For example a window has an equal thickness in the x-direction and a wedge of 2λ in the y direction. If this window is tilted in the x direction, then the angle of the sum phasor $E_{g1} + E_{g2}$ varies with the y direction by 12π, but the angle φ between the two phasors does not vary with the y direction, and remains unchanged. Therefore if $\varphi \neq$ oddπ, then the resulting wave front shows 6 horizontal fringes, i.e., a ripple of 6 cycles in the y direction. On the other hand, if the RF is tilted such that $\varphi =$ oddπ, then E_{g1} and E_{g2} cancel each other, as if there were no multiple reflections.

Because $\epsilon \ll \theta \ll 1$ in most cases, φ from Eq. (8) can be approximated by $4dk\theta\epsilon/n$, where θ and ϵ are in radians. The condition of $\varphi = m\pi$ is of most interest for minimizing (for $m =$ odd) or maximizing (for $m =$ even) the effect of multiple reflections. Using the above approximation, we obtain $4dk\theta\epsilon/n = m\pi$, for θ and ϵ in radians. Therefore the phase error is either zero or maximum when the tilt angles θ and ϵ satisfy one of the following conditions:

$$d\theta\epsilon/\lambda n \approx \text{odd} \times 0.000406, \quad \text{for error} = 0, \tag{9}$$

$$d\theta\epsilon/\lambda n \approx \text{even} \times 0.000406, \quad \text{for error (p–v)} \approx 2r^2/\pi, \tag{10}$$

where the error is in fringes, θ and ϵ are in degrees, d is in millimeters, λ is in nanometers, and r is the coefficient of reflection. From Eqs. (9) and (10), if $n = 1.5$ and $\lambda = 633$ nm, then $d\theta\epsilon \approx 0.386m$, where m is a natural number. The results of this equation for $m = 1$ and 2 correspond to those in Table 1 for $\varphi = \pi$ and 2π, respectively. This approximation reveals the inversely proportional relationship among d, θ, and ϵ and is convenient for estimating the proper tilt angles for the window and the RF. If $\epsilon \approx \theta \ll 1$, φ in Eq. (8) can be approximated by $2dk(2\theta - \epsilon)\epsilon/n$, where θ and ϵ are in radians.

Table 1. Values of φ and L for Different Tilt Angles θ and ϵ (in Degrees) for a Window Thickness of 10 mmn or 20 mm and a Refractive Index of 1.5 at 633 nm

	ϵ			
θ	$d = 10$ mm	$d = 20$ mm	φ	L
—	0	0	0	$2r^2s$
0.5	0.06853	0.03633	π	0
0.5	0.12474	0.06853	2π	$2r^2s$
1	0.03756	0.01912	π	0
1	0.07266	0.03756	2π	$2r^2s$
2	0.01930	0.00970	π	0
2	0.03825	0.01931	2π	$2r^2s$

Experiment

In the experiment, a laser phase-shifting Fizeau interferometer was used, as shown in Fig. 5. The source is an HeNe laser at 633 nm. The transmission flat (TF) has a clear aperture 15 cm in diameter and can be displaced along the ray direction with a piezoelectric transducer to introduce the proper phase shift. The two coordinate systems in the RF and the detector indicate the relationship between the window and the intensity pattern on the detector. In both coordinate systems, the x direction is in the

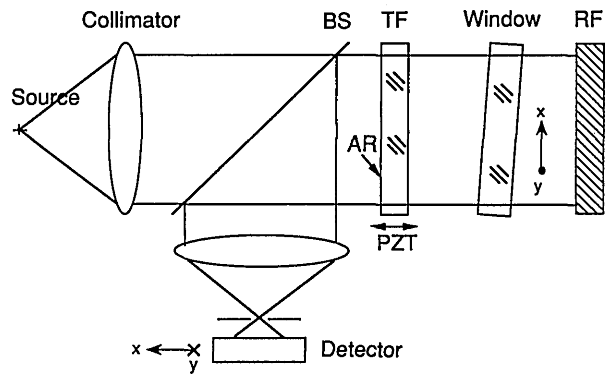

Fig. 5. Top view of laser phase-shifting interferometer. Source, HeNe at 633 nm; BS, beam splitter; TF, transmission flat (fused silica); RF, return flat (fused silica); AR, antireflection coating; PZT, pizoelectric transducer.

plane of the paper, and the y direction is normal to plane of the paper. Both RF and TF are fused silica. The window is a BK7 plate (20 mm thick and 150 mm in diameter) with a wedge angle of 1.725 arcsecs. If this wedge is oriented in the vertical direction, it can be shown that this window introduces 6 horizontal fringes in the transmitted wave front.

First we look at the intensity pattern of the sum of the three returned rays, $E_t + E_{g1} + E_{g2}$, by removing the TF from Fig. 5. The window is tilted such that no direct reflections from the front and the rear surfaces of the window enter the detector. The tilt orientation of the window can be categorized into two cases: (a) perpendicular to the window wedge direction and (b) parallel to the window wedge direction. For convenience, we orient the window such that its wedge is in the y direction and the window is tilted in either the x direction or the y direction. For case (a), the window is tilted $\theta = 0.5°$ in the x direction. Figure 6 shows the intensity patterns when the RF is not tilted in the x direction, $\epsilon = 0°$, or when the RF is tilted in the x direction, $\epsilon = 0.03633°$, respectively. In Fig. 6(a), the intensity pattern has faint but obvious horizontal interference (ghost) fringes. In Fig. 6(b), these ghost fringes disappear. These two tilt angles correspond to $\varphi = 0°$ and π, respectively, as given in Table 1 for $d = 20$ mm. Increasing the tilt of the RF to 0.06853°, these ghost fringes reappear. In case (b), the window is tilted in the y direction ($\theta = 0.5°$). In this case, the window tilt direction is parallel to the window wedge direction. When the RF is not tilted in the y direction, $\epsilon = 0°$, or when the RF is tilted in the y direction, $\epsilon = 0.03633°$, respectively, we obtain the same results as those in Fig. 6. From both Figs. 6(a) and 6(b), as long as the RF is tilted in the same plane as that for the filt of the window, the interference ghost fringes can disappear easily, regardless of the orientation of the wedge of the window. On the other hand, whenever $\epsilon = 0°$, the interference ghost fringes cannot be removed.

To measure the phase of the resulting wave front of the three return rays, $E_t + E_{g1} + E_{g2}$, the TF is put back into the interferometer. Figure 7 shows the intensity patterns corresponding to those in Fig. 6, when the TF is tilted to give several vertical fringes. The wedge is in the y direction, and the window is tilted 0.5° in the x direction. In Fig. 7(a), it is clear that there are several vertical main fringes and six ghost horizontal fringes are the same as those in Fig. 6(a). On the other hand, when the RF is tilted 0.03633° in the x direction, the ghost fringes disappear as shown in Fig. 7(b). Figure 8 shows the cross-sections in the y direction of the two measured wave fronts obtained from Fig. 7. In Fig. 8(a), the ripples correspond to the ghost fringes in Figs. 6(a) and 7(a). The peak to valley of the phase error caused by the multiple reflections is about 0.025λ. In Fig. 8(b), there is no evidence of ripples.

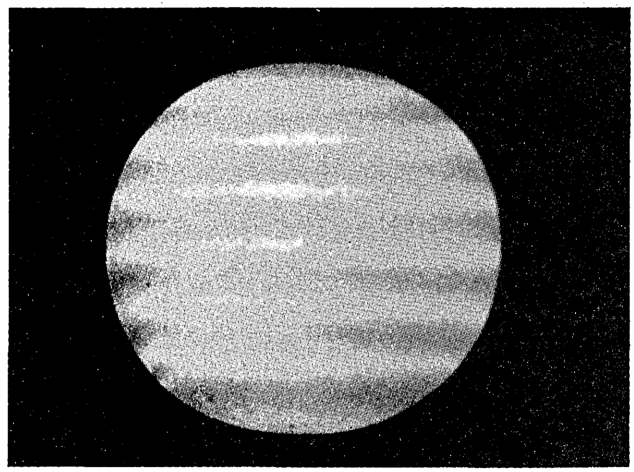

(a)

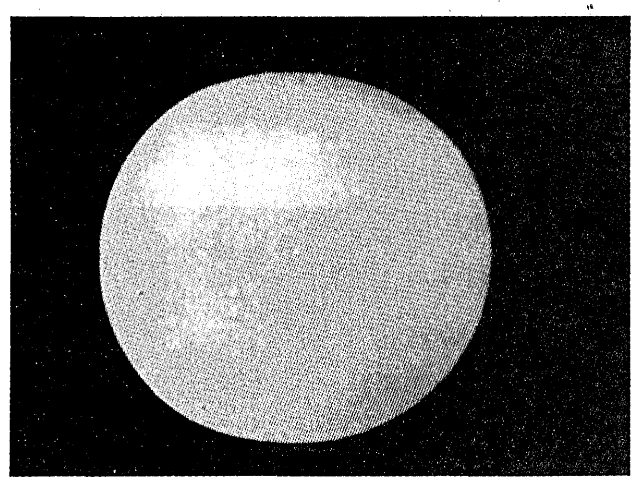

(b)

Fig. 6. Intensity patterns obtained with RF and a window. The window has a wedge in the y direction and is tilted in the x direction ($\theta = 0.5°$). In (a) the RF is not tilted in the x direction, and in (b) the RF is tilted 0.03633° in the x direction.

Figure 9 shows the intensity distribution maps of a 12 cm × 8 cm thin fused-silica plate. The maps are obtained using the same interferometer in Fig. 5 without a TF, for different tilt angles of RF. In Fig. 9(a), the RF is not tilted, and there are several curved ghost fringes that are a fixed pattern caused by the multiple reflections. It should be noted that these

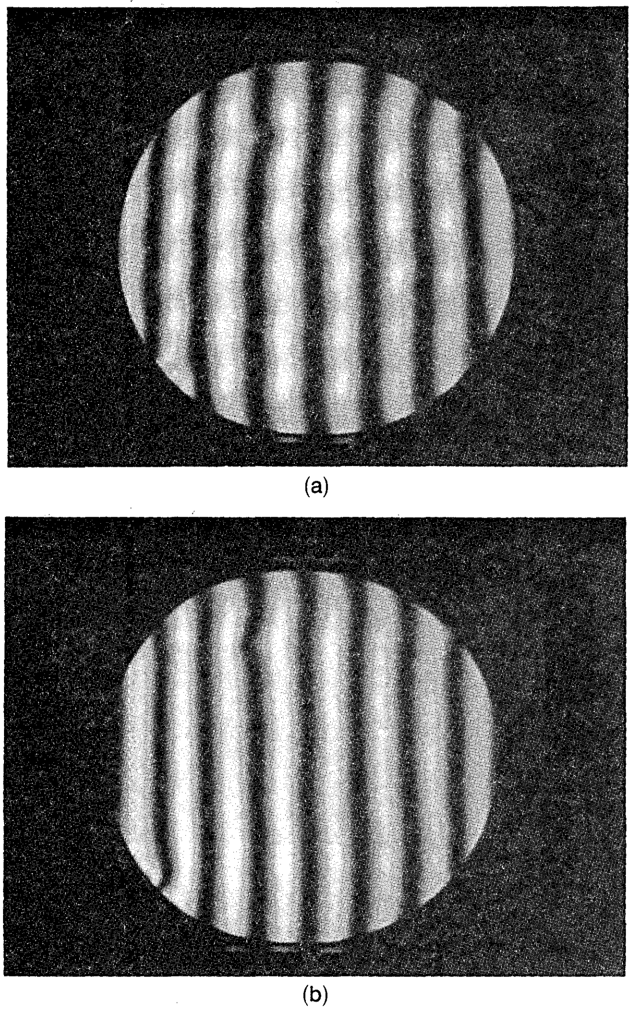

Fig. 7. Intensity patterns corresponding to those in Fig. 6, when the TF is tilted to give several vertical fringes. In (a) the RF is not tilted, and in (b) the RF is tilted properly.

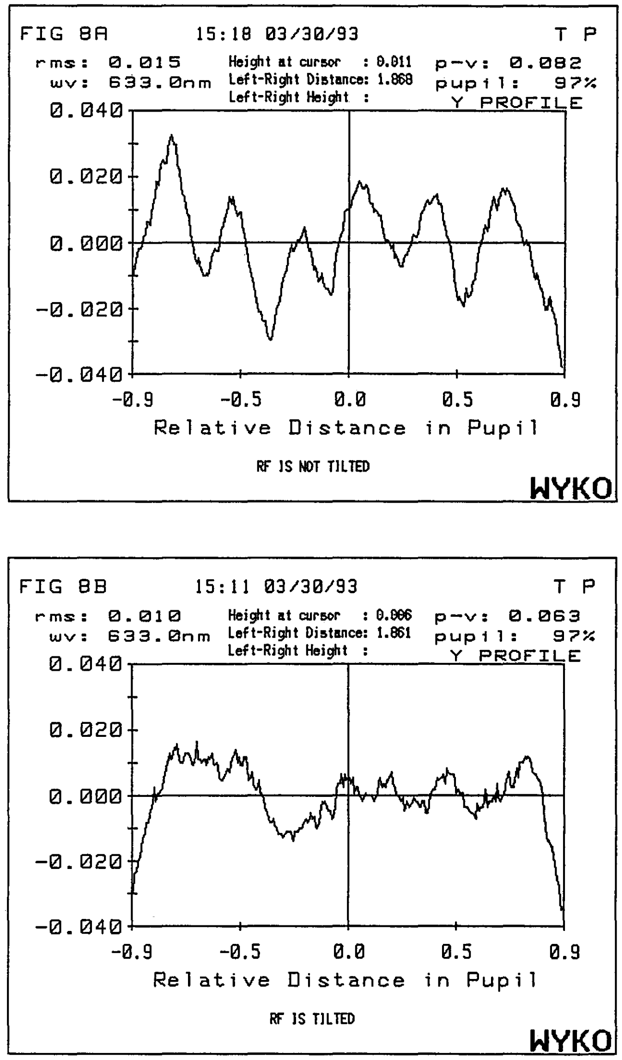

Fig. 8. Cross-sections in the y-direction of the two measured wave fronts obtained from Fig. 7. In (a) the RF is not tilted, and in (b) the RF is tilted properly.

ghost fringes bend sharply around the boundary of the plate because of the rapid thickness variation at the edges. On the other hand, when the RF is properly tilted, the ghost fringes disappear, as shown in Fig. 9(b). Then the TF is put back into the interferometer and is tilted to give several horizontal fringes. Figure 10(a) is the intensity pattern when the RF is not tilted, and there are several horizontal main fringes and some ghost fringes that are the same as those in Fig. 9(a). Figure 10(b) is the intensity pattern when the RF is tilted properly and the ghost fringes disappear.

Discussion

When a window is tested, the cavity formed by the TF and the RF is almost always measured first, and then the window is inserted into the cavity. Typically both the TF and RF are adjusted such that the ray is normal with respect to them. Because the wedge angle (e.g., 5 arcsec) is so small, after inserting the window the ray is still normal to the RF (i.e., $\epsilon = 0°$). Therefore the measured wave front always shows an error of ripple, no matter what the thickness and the tilt of the window may be. As shown in Figs. 6(a) and 7(a), whenever the RF is normal to the rays, the error caused by the multiple reflections is maximum. To remove the effect of multiple reflections, the RF must be tilted by an angle in either the same direction as or the opposite direction from that for the tilted window, as explained below.

Figures 6(b) and 7(b) clearly show that the effect of multiple reflections is eliminated when the RF is tilted properly by the same angles as derived from Eq. (9). It should be noted that not only the angle but also the direction of tilt is important. For convenience, we define the tilt direction by the change of the normal of the tilted surface before and after the tilt. Therefore tilting in the x direction means the normal of the surface moves in the x direction. If the tilt direction of the RF is not parallel to that of the window, there is an angle between those two directions. The new incident angle of the ray reflected by the RF is equal to the magnitude of the vector difference of these two tilts. For $\epsilon \ll \theta \ll 1$, if the

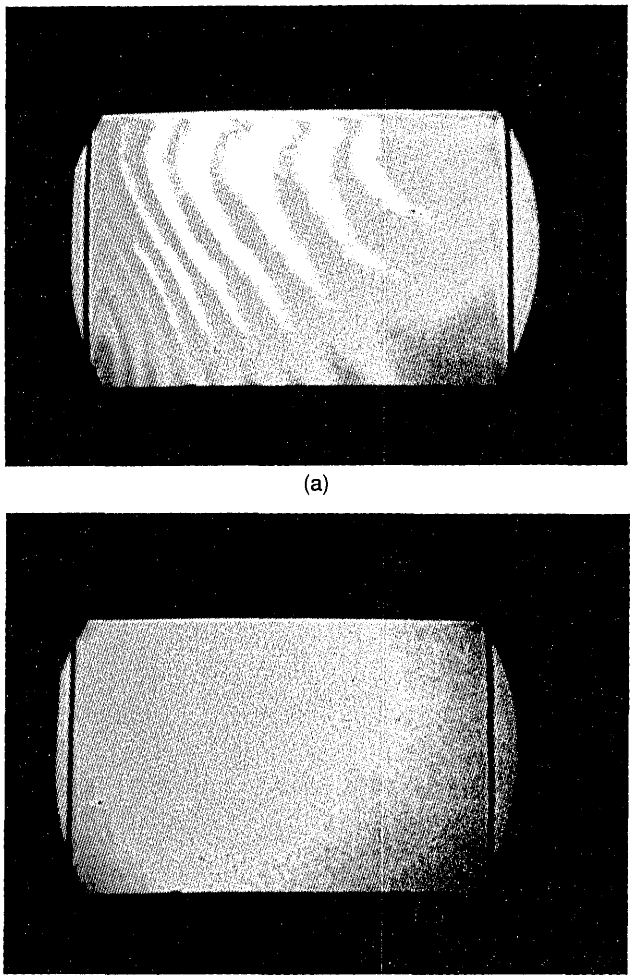

(a)

(b)

Fig. 9. Intensity patterns obtained with RF and a thin fused silica window. In (a) the RF is not tilted, and in (b) the RF is properly adjusted.

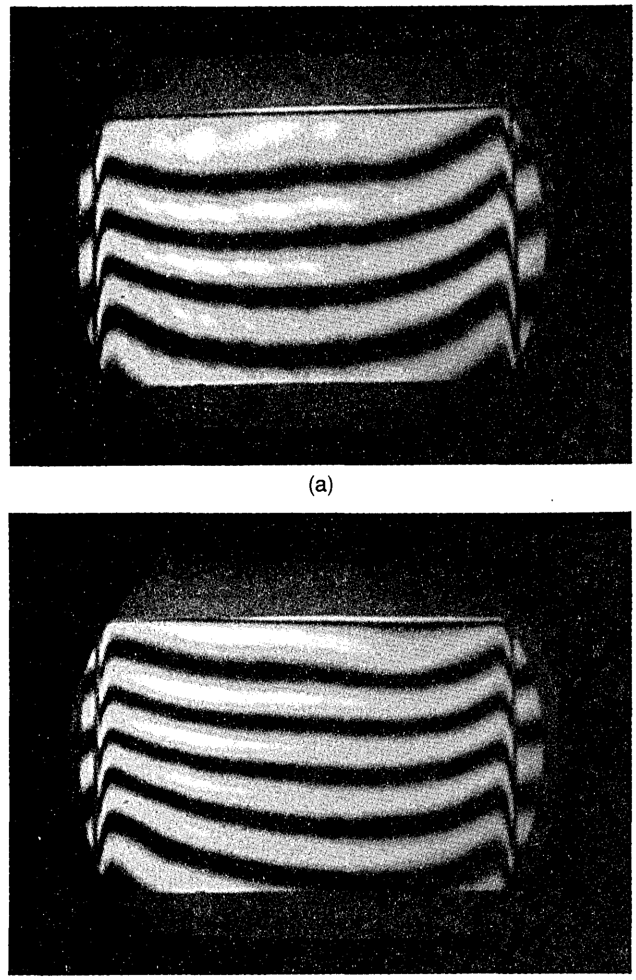

(a)

(b)

Fig. 10. Intensity patterns corresponding to those in Fig. 9, when the TF is tilted to give several horizontal fringes. In (a) the RF is not tilted, and in (b) the RF is tilted properly.

two directions are perpendicular, then the new incident angle is almost equal to the original one. Hence the tilt of the RF has no effect, and the ghost fringes do not disappear in this situation. In the experiment, it can be easily shown that when the tilts of the window and the RF are in perpendicular directions (such as one in the x direction and the other in the y direction), the ghost fringes do not disappear.

In the derivation of Eqs. (8)–(10), we assume that the walk-off is negligible or that the window has an equal optical thickness for the two locations separated by the walk-off distance. A simple situation is that the material of the window is uniform and the two surfaces are absolutely flat. This equal optical thickness condition can be achieved by tilting both the window and the RF in a direction (x direction) perpendicular to the orientation of the wedge (y direction), e.g., case (a). In fact, what is important is that the difference of the optical thickness for two points separated by the walk-off distance needs to be constant. A constant change of the optical thickness is equivalent to adding a constant angle between phasors E_{g1} and E_{g2}. This is equivalent to the case where the tilt of the window is parallel to the wedge direction of the window, as shown in case (b). If the material of the window is uniform and the two surfaces are absolutely flat, then the thickness difference, resulting from a wedge, over the walk-off distance is equal to a constant τ_0, i.e., $d(x', y) - d(x, y) = \tau_0$. From Eq. (6),

$$\varphi = 2nkd(x, y)\{[1 - \sin^2(\theta)/n^2]^{1/2} - [1 - \sin^2(\theta - 2\epsilon)/n^2]^{1/2}\} - 2nk\tau_0. \quad (11)$$

For certain θ and ϵ values, the condition of $\varphi = \pi$ can be achieved. This is why the ripples can disappear when the tilt of the window is parallel to the wedge direction of the window.

In reality, the optical thickness in both the x and y directions could vary. If the material of the window is not uniform or the two surfaces are not absolutely flat, then the difference of $d(x', y) - d(x, y)$ varies over the pupil, i.e., $d(x', y) - d(x, y) = \tau_0 + \Delta\tau$, where $\Delta\tau$ is the optical thickness variation minus the nominal wedge height over the walk-off distance (i.e., $x' - x$).

Equation (6) becomes

$$\varphi = 2nkd(x, y)[1 - \sin^2(\theta)/n^2]^{1/2} - 2nk[d(x, y) + \tau_0 + \Delta\tau][1 - \sin^2(\theta - 2\epsilon)/n^2]^{1/2}. \quad (12)$$

By tilting the window and the return flat (θ and ϵ), we can obtain the following condition:

$$2nkd(x, y)[1 - \sin^2(\theta)/n^2]^{1/2} - 2nk[d(x, y) + \tau_0] \times [1 - \sin^2(\theta - 2\epsilon)/n^2]^{1/2} = \pi, \quad (13)$$

and hence Eqs. (12) and (7) become

$$\varphi = \pi - 2nk\Delta\tau \times [1 - \sin^2(\theta - 2\epsilon)/n^2]^{1/2} \approx \pi - 2nk\Delta\tau, \quad (14)$$

$$\text{phase error (p–v)} = |\sin^{-1}[2r^2 \cos(\pi/2 - nk\Delta\tau)]/\pi| \approx |2r^2nk\Delta\tau/\pi|, \quad \text{in fringes} \quad (15)$$

respectively. Because the walk-off distance is constant, $\Delta\tau$ is equivalent to the walk-off distance times the difference between the slope of the optical thickness in the walk-off direction and the nominal slope in the same direction. For a small walk-off distance or for smooth surfaces, the typical value of $\Delta\tau/\lambda$ is much less than 0.01, and hence $\varphi \approx \pi$ and the phase error caused by $\Delta\tau$ is negligible. Therefore even if the thickness difference for two points over the walk-off distance varies slightly over the pupil, the ghost fringes can disappear when the tilt angles are adjusted properly. For example the window used in the experiment has several curved fringes, as shown in Fig. 9a. This indicates that the window has a wedge approximately in the x direction, and the optical thickness is not the same in all directions (showing curved fringes). For this window, we are still able to remove the effect of multiple reflections, as shown in Figs. 9b and 10b.

To effectively remove the ghost fringes, we propose the following procedure for a Fizeau interferometer. This procedure can also be applied to a Twyman-Green interferometer, where the reference mirror is equivalent to the TF:

1. Tilt the TF by a large angle to avoid the complexity. Adjust the RF such that it is normal to the collimated beam.
2. Insert the window into the cavity, and orient the wedge in one direction. Choose a proper tilt angle θ for the window. Tilt the window at this angle in any direction. (Tilt in the direction that gives the smallest $\Delta\tau$, e.g., perpendicular to the wedge direction, is preferred, but it is not critical.) An intensity pattern with a faint interference pattern can be observed, such as in Fig. 6(a).
3. Tilt the RF in the same direction as or the opposite direction from that for the tilted window. The faint interference pattern in step 2 disappears and then appears repeatedly when the tilt angle increases. The angle corresponding to the first disappearance of the interference pattern should be chosen because it introduces the smallest walk-off. This tilt angle corresponds to ϵ in Eq. (9) for odd = 1.
4. Adjust TF to form the main interference fringes.

When the fixed pattern has several fringes, the disappearance of the fringes in step 3 is obvious, and this procedure is easy to follow. However, if the wedge angle is so small and the surfaces are so flat that the ghost interference pattern is about one fringe or less in step 2, then it might be difficult to observe the disappearance of the fringe in step 3. For this case, the angles of θ and ϵ need to be measured accurately. One should note that after the window is inserted, the collimated beam is slightly tilted because of the wedge and is no longer normal to the RF. Moreover, tilting the TF may also cause the collimated beam to change its direction slightly, because some TF's have a wedge. These make the measurement of ϵ more difficult, because the tilt angle ϵ is measured with respect to the transmitted collimated beam direction.

In all, when the tilt angles of the RF and the window are properly adjusted, and both are tilted in the same plane, the interference ghost fringes can be removed effectively, regardless of the orientation of the wedge of the window and the fringes patterns, as shown in Figs. 6–10. Moreover, a smaller walk-off gives a smaller $\Delta\tau$ and hence a smaller error. Similarly, a smaller lateral displacement introduces a smaller error. To ensure that the lateral displacement and the walk-off distance are small, one needs to tilt the window at an angle that is just enough to keep the ray from entering the interferometer and also to place the RF close to the window.

Conclusion

When an optical window is being tested, a collimated beam is transmitted through the window and then is reflected back by a return flat (RF). The window is always tilted and the incident angle to the window is not zero. If the RF is tilted slightly, the reincident angle of the ray reflected by the RF is different from the original incident angle. To effectively remove the ghost fringes, one needs to tilt the RF in the same plane as that for the tilt of the window, regardless of the orientation of the wedge of the window. We have shown that the effect of multiple reflections of the window can be removed by tilting both the window and the RF properly. This method allows us to measure a window with a small wedge angle of several arcseconds, without using antireflective coatings on both surfaces.

References

1. J. H. Bruning, J. E. Gallagher, D. P. Rosenfeld, A. D. White, D. J. Brangaccio, and D. R. Herriott, "Digital wave front measuring interferometer for testing optical surfaces and lenses," Appl. Opt. **13,** 2693–2703 (1974).

2. J. Schwider, R. Burow, K.-E. Elssner, J. Grzanna, R. Spolaczyk, and K. Merkel, "Digital wave-front measuring interferometry: some systematic error sources," Appl. Opt. **22,** 3421–3432 (1983).
3. P. Hariharan, "Digital phase-stepping interferometry: effects of multiply reflected beams," Appl. Opt. **26,** 2506–2507 (1987).
4. C. Ai and J. C. Wyant, "Effect of spurious reflection on phase shift interferometry," Appl. Opt. **27,** 3039–3045 (1988).
5. G. Bonsch and H. Bohme, "Phase-determination of Fizeau interferences by phase-shifting interferometry," Optik **82,** 161–164 (1989).
6. R. A. Nicolaus, "Evaluation of Fizeau interferences by phase-shifting interferometry," Optik **87,** 23–26 (1991).
7. C. Ai and J. C. Wyant, "Effect of retroreflection on a Fizeau phase-shifting interferometer," Appl. Opt. (to be published).